Incorporation of Aluminium Guest-ions in Nominally Alumina-free Calcium Silicate Hydrates: Effects on Crystal Structure and Thermal Stability

N. Meller[1], C. Hall[1], K. Kyritsis[1], G. Giriat[1], H. J. Jakobsen[2], J. Skibsted[2]

[1]The Centre for Science at Extreme Conditions, The University of Edinburgh, Edinburgh, UK; [2]Instrument Centre for Solid-State NMR Spectroscopy, Department of Chemistry, University of Aarhus, Aarhus, Denmark

1. Introduction

Specialised cement formulations are used as sealants for both oilfield and geothermal wells where the temperature exceeds 110 °C. Below this temperature oilwell cements are sufficiently durable while above it the predominant phase formed in an oilwell cement, α-dicalcium silicate hydrate α–C_2SH (C=CaO, S=SiO_2, A=Al_2O_3, H=H_2O, $\overline{C}$=CO_2), is too weak and permeable to seal the well [1, 2]. Therefore silica is commonly added to cement (~ 0.35 BWOC) to reduce the C/S ratio to about 1.0. This prevents the formation of α–C_2SH and instead a sequence of calcium silicate hydrates with sufficient strength and impermeability form over a range of temperatures [3]. At temperatures above 110 °C 11Å tobermorite $C_5S_6H_5$ forms and converts to xonotlite C_6S_6H or gyrolite $C_8S_{12}H_2$ at 160 °C, depending on the amount of silica added. At 250 °C truscottite $C_{14}S_{24}H_6$ forms at the expense of gyrolite whereafter it co-exists with xonotlite until 400 °C. While these formulations are normally acceptable for oilwells, they are not always durable in the hostile chemical environments encountered in geothermal wells thus formation damage, sealant damage or deterioration can occur.

Recently, our work has focussed on designing cements with the addition of new additives (e.g. Al_2O_3) not commonly used in well formulations [4-6], employing an original idea by Barlet-Gouédard et al. [7]. It has become apparent that whilst the addition of alumina can lead to the formation of Al-bearing phases such as hydrogarnet, $C_3AS_{3-x}H_{2x}$ (x = 1-3), this is not always the case. Nominally Al-free calcium silicate hydrate phases, e.g. 11Å tobermorite, xonotlite and gyrolite are frequently observed in samples synthesised from oilwell cement, silica and alumina. In the absence of amorphous material in our samples, it may be assumed that the alumina is residing in the calcium silicate hydrate phases and this is the subject of our paper.

Naturally occurring calcium silicate hydrates frequently contain aluminium guest-ions [8-10] and laboratory syntheses of tobermorite suggest it can

be stabilised above its normal stable temperature of 150 °C by aluminium [11-17]. It is also noted that 11Å tobermorite is the least permeable and strongest of the calcium silicate hydrates [11, 18] and thus it is the most suitable phase to be present in a well sealant. However its structure is altered by the presence of alumina from the anomalous form [19], which retains its 11Å spacing on heating, to the normal form which typically collapses to 9Å tobermorite C_5S_6H at 300 °C in air [14]. This could have serious implications as to doped tobermorites may not be ideal as well sealant materials if they exhibit weaker crystal structures.

In this study we have synthesised Al-free calcium silicate hydrates to establish the stable phase assemblage and to obtain a valuable basis from which to examine the effects of aluminium doping. Once the mineral assemblages are established using X-ray diffraction and scanning electron microscopy, the short-range order is investigated by solid-state NMR spectroscopy to determine the location of aluminium in the C-S-H phases and the degree of ordering.

2. Synthesis of samples for laboratory powder diffraction and NMR spectroscopy

Lime CaO (Sigma Aldrich) was initially chosen as the calcium component, however, it typically contains a few wt% carbonate which contaminated the final product with either calcite $C\overline{C}$ or scawtite $C_7S_6\overline{C}H_2$. Calcining the lime eliminated the presence of carbonate but dramatically reduced the reactivity and subsequent milling did not significantly increase this. Hence alternative calcium sources were explored to minimise carbonate contamination. Portlandite CH (Riedel-de-Haën) and monoclinic tricalcium silicate C_3S (Construction Technology Laboratories, Skokie, IL) do contain less initial carbonate but produce different product phases. Silica SiO_2 is added as either quartz (Fluka) or amorphous silicic acid (Sigma Aldrich) but again both reagents give different product phases although the differences are more subtle than those observed for the calcium-based reagents (*vide infra*). Once the stable calcium silicate hydrates were established, small amounts of corundum αAl_2O_3 (Buehler) were added in an attempt to form phases that would be stable at higher temperatures than normally observed.

Slurries were mixed with water (w/s=2 to 3) and placed in steel cups, 3cm dia by 1cm. Seven steel cups were then sealed in 125 mL capacity stainless steel pressure vessel (Parr Instruments, type 4750) and heated for 5 days. Sufficient excess water is present that the samples are cured under saturated vapour pressure (RH = 100%) conditions throughout the experiment. Once cured the Parr Cell is removed from the oven, chilled rapidly in cold water to prevent further reaction and the samples removed from the Parr Cell and placed in a vacuum desiccator to minimise

carbonation. Dry samples were analysed by X-ray diffraction (XRD) to determine mineralogy and nuclear magnetic resonance (NMR) to characterise the location of aluminium guest-ions in the calcium silicate hydrate structures.

3. Laboratory powder X-ray diffraction

A Bruker-AXS D8-Series 2 X-ray powder diffractometer, running at 40kV and 40mA, was employed. Incident Cu K-α radiation was used with a Ge monochromator and passed through a 2 mm monochromator exit slit and 0.2° divergence slit. A Braun position sensitive detector was used to collect data. Diffraction patterns were collected over an angular range of 5 to 70° 2θ for approx 30 min total time using a step size of 0.014° 2θ and a count time of 0.3° 2θ per step.

3.1. Lime and silica

Quartz was added to lime and the resulting phases after 5 days are shown in Fig. 1. Phases formed at 200 °C are portlandite, hillebrandite C_2SH, foshagite C_4S_3H, xonotlite, 11Å tobermorite, gyrolite, and quartz (Fig 2). The 11Å tobermorite is not observed in samples cured at 250 °C which include kilchoanite C_6S_4 and truscottite. Carbonation of samples produces calcite and scawtite (Fig. 2) but exactly which phases are converted is uncertain.

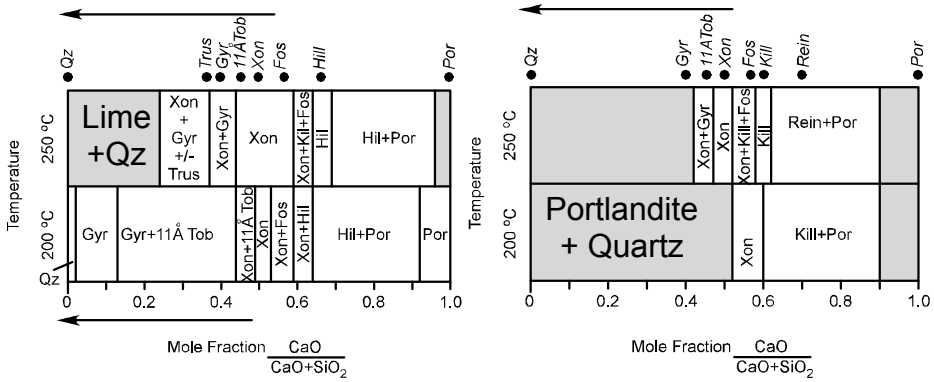

Fig. 1. Phase assemblages resulting from the synthesis of lime or portlandite and quartz at 200 and 250 °C. Arrows indicate the presence of unreacted quartz. Mole fraction $CaO/CaO+SiO_2$ for the individual phases is shown along the top of the diagram. Key: Qz=quartz, Trus= truscottite, Gyr=Gyrolite, Xon=xonotlite, Kil=kilchoanite, Kill=killalaite, Fos=foshagite, Hil=hillebrandite, Rein=reinhardbraunsite, Por=portlandite.

Whilst the observation of some phases (e.g. hillebrandite, xonotlite, gyrolite) is in agreement with previous investigations, there are some discrepancies. The work of Taylor [3] and Hong and Glasser [20] seem to be the most complete and comprehensive, Taylor giving details of phases formed over the temperature range 50 to 1000 °C and Hong and Glasser

covering the range 0 to 220 °C. Hence they will be used as the primary sources of comparison. At the low silica side of the lime-quartz phase diagram jaffeite $C_6S_2H_3$, not present in Fig. 1, is observed at 200 °C by Hong and Glasser and above 200 °C by Taylor. The presence of foshagite agrees well with the stability field reported by Hong and Glasser but lies approximately 50 °C below that of Taylor. Kilchoanite forms at even lower temperatures (250 °C vs 600 °C) and the reasons for these discrepancies are not yet clear.

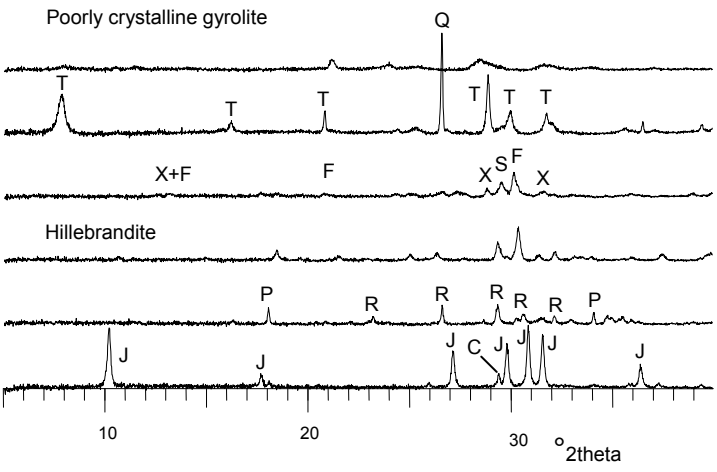

Fig. 2. XRD patterns for selected samples to illustrate the presence of different phases. From the bottom samples are:
C_3S/200 °C
portlandite+quartz/250 °C
lime+silicic acid/200 °C
lime+quartz/200 °C
lime+quartz/200 °C
lime+silicic acid/200 °C

Key: J=jaffeite, C=calcite, P=portlandite; R=reinhardbraunsite, F=foshagite, X=xonotlite, S=scawtite, T=11Å tobermorite, Q=quartz.

11 Å tobermorite usually converts to xonotlite and gyrolite above 160 °C and is hence not observed at 200 °C in previously published phase diagrams. Outwith the stability field tobermorite persists but as a metastable phase and, over time, it will convert to xonotlite [16]. As no variable curing times were used in this study this cannot yet be commented on but may well be an explanation as to why we observe tobermorite at 200 °C when existing phase diagrams show this to be well above its normal stability field.

The presence of truscottite is not obvious in this system, gyrolite preferring to form instead. Taylor suggests that truscottite forms above 200 °C so we would expect to see it. However, Hong and Glasser do not observe this phase either, suggesting its stability field may need adjusting. Moreover, when quartz is replaced by amorphous silica, truscottite becomes more abundant (Fig. 2), suggesting the starting products control the rate of reaction if not the final phase assemblage.

3.2. Portlandite and quartz

The addition of portlandite instead of lime produces two additional phases, killalaite C_6S_4H and reinhardbraunsite C_5S_2H (Fig. 1), killalaite being

observed at both 200 and 250 °C. The stability of this phase is not detailed by Taylor but Garbev et al. [21] suggest killalaite is the lower temperature form of kilchoanite. If the phase diagrams are compared this does not make sense as both killalaite and kilchoanite form at 250 °C, killalaite being formed when portlandite is the calcium source and kilchoanite when lime is used. The presence of both phases in quite clearly defined systems (i.e. portlandite vs lime) also suggests the presence of killalaite is not an artefact of e.g. kilchoanite converting to killalaite on cooling.

Reinhardbraunsite, commonly observed when synthesizing cement and silica samples at 250 °C and above, is observed in the portlandite quartz system. Taylor reports the lower stability limit of this phase as over 300 °C, however, our results agree well with other reports on the formation of reinhardbraunsite at lower temperatures [21-24].

3.3. Tricalcium silicate

A few samples of C_3S were cured at 200 °C to ascertain whether the hydration products would be the same as for the lime or portlandite and silica systems. C_3S on its own readily hydrates to jaffeite (Fig. 2), in agreement with earlier observations for both pure C_3S [25] and cement-based systems [5]. However, the formation of jaffeite is apparently uncommon in either lime/portlandite based systems or those based on C_2S at 200 °C. C_2S does produce jaffeite but only at temperatures above 200 °C using specialised high temperature mixing methods [22].

Increasing the C/S ratio by addition of portlandite to C_3S results in the formation of jaffeite and portlandite. When silica is added in the form of quartz to lower the C/S ratio 11Å tobermorite, xonotlite and gyrolite are formed. Again, the formation of xonotlite and gyrolite are in accordance with previous work but tobermorite is metastable.

3.4. Addition of alumina

Alumina in the form of corundum was added to both the lime-quartz and the portlandite-quartz systems (Fig. 3). In both cases the addition of alumina stabilises tobermorite to 250 °C as previously observed [11, 14-17]. The question of whether the Al-doped tobermorite is stable in the long term is currently unknown. Whilst outside its normal stability field by as much as 100 °C in the calcium silicate hydrate system, it may well be that the presence of alumina changes the phase boundaries of this system. The phase diagrams presented in Fig. 3 are our first attempt to incorporate the effect of aluminium guest-ions on the phase stabilities. 11Å tobermorite is not the only phase forming in the presence of alumina, kilchoanite and xonotlite are also present. In one sample, tobermorite is not observed, suggesting the alumina must be residing in one or both of

xonotlite and kilchoanite. This is not an unreasonable assumption as guest ions are frequently observed in natural C-S-H samples [8-10]. Furthermore, samples synthesised from real cements are sometimes

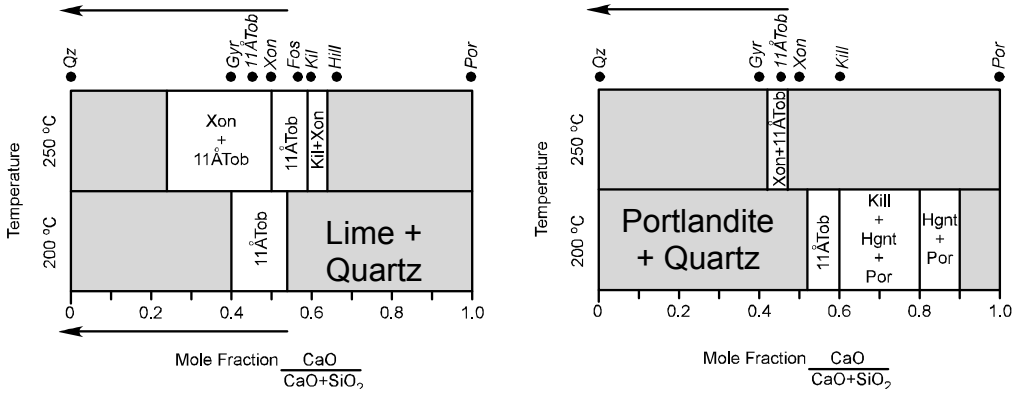

Fig. 3. Phase assemblages resulting from synthesis of quartz and either lime or portlandite and 0.05 Al_2O_3 (BWOS) at 200 and 250 °C. Arrows indicate the presence of unreacted quartz. Mole fraction CaO/[CaO+SiO_2] of individual phases is shown along the top of the diagram while arrows indicate the presence of unreacted quartz. Key: Qz=quartz, Trus=truscottite, Gyr=Gyrolite, Xon=xonotlite, Kil=kilchoanite, Kill=killalaite, Fos=foshagite, Hil=hillebrandite, Rein=reinhardbraunsite, Por=portlandite.

observed to contain xonotlite as the only crystalline phase, suggesting it must contain ions other than calcium, silicon, oxygen and hydrogen.

The preliminary data show that foshagite is absent when a small amount of alumina is added to either the lime or portlandite system. Previous work by Meller et al. [5] has shown that in real cement systems cured at 200 °C, foshagite is not observed. Alumina, indeed other ions also, are commonly present in cement and their presence may actively inhibit the formation of foshagite.

4. ^{27}Al and ^{29}Si MAS NMR spectroscopy

The ^{27}Al and ^{29}Si MAS NMR spectra were recorded on Varian INOVA 600 (14.1 T) and -400 (9.4 T) spectrometers, respectively, using homebuilt CP/MAS NMR probes for 4 and 7 mm o.d. rotors, and the optimized experimental conditions for ^{27}Al and ^{29}Si MAS NMR studies of cementitious materials described earlier [26, 27]. Isotropic chemical shifts are relative to 1.0 M $AlCl_3 \cdot 6H_2O$ and tetramethylsilane (TMS). The NMR analyses focus on: portlandite–quartz–alumina and lime–quartz–alumina samples cured at 250 °C; and Portland cement including 0.5 silica flour BWOC and 0.17 alumina BWOC cured at 200 °C, all employing corundum as the alumina source.

The formation of 11Å tobermorite in samples doped with alumina is supported by the corresponding ^{29}Si MAS NMR spectra (Fig. 4) which all include resonances that can be assigned to the different silicate species in 11Å tobermorite, i.e., Q^1: -81.0 ppm, Q^2(1Al): -83.5 ppm, Q^2: -86.0 ppm,

Q^3(1Al): -92.0 ppm, Q^3: -96.6 ppm, in accordance with earlier studies of synthetic 11Å tobermorites [28-30]. For the Portland cement sample these resonances are present with nearly the same intensities as observed for a natural sample of 11-Å tobermorite while the resonances from the Q^2 and Q^3 sites (-86.0 and -96.6 ppm) exhibit somewhat increased intensities for the portlandite and lime samples. This reflects the fact that these samples also include minor quantities of xonotlite which includes two Q^2 and one Q^3 sites with resonances at -86.4 ppm, - 87.2 ppm, and -97.6 ppm [31]. The ^{27}Al MAS NMR spectra (Fig. 4) display resonances from two different AlO_4 sites with centres of gravity of 64 ppm and 56 ppm which can be assigned to Al guest-ions incorporated in the silicate network of 11Å tobermorite. Moreover, a resonance at 15 ppm is observed which originates from minor quantities of unreacted corundum in the samples. In fact, the largest intensity for this peak is observed for the Portland cement sample which employed 0.10 Al_2O_3 (BWOS) as compared to 0.05 (BWOS) for the two other samples. The ^{29}Si and ^{27}Al MAS NMR spectra in Fig. 4 independently show the incorporation of Al guest-ions in the silicate network for 11-Å tobermorite. The indirect detection of the Al ions by their effect on neighbouring SiO_4 tetrahedra in the ^{29}Si MAS NMR spectra, i.e., the observation of Q^2(1Al) and Q^3(1Al) sites, suggests that Al is incorporated in the bridging sites of the silicate chains and in double-chain bridging sites. This is in accordance with the two tetrahedral AlO_4 sites observed by ^{27}Al MAS NMR and an earlier reported assignment by Gabrovsek et al [29].

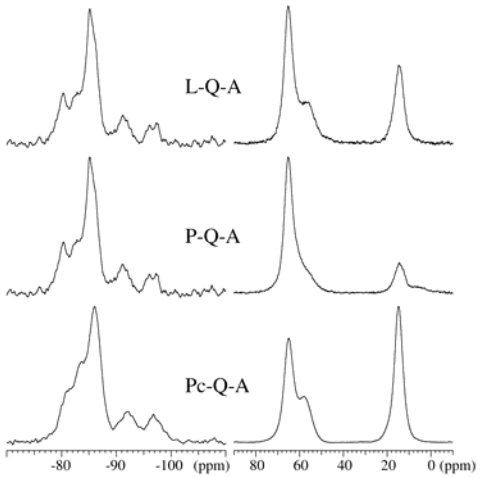

Fig. 4 ^{29}Si and ^{27}Al MAS NMR spectra (left and right column, respectively) of the lime–quartz–alumina (L-Q-A) and portlandite–quartz–alumina (P-Q-A) samples cured at 250 ^{o}C and the Portland cement–quartz–alumina (Pc-Q-A) sample cured at 200 ^{o}C. The ^{29}Si MAS NMR spectra employ a spinning speed of ν_R = 6.0 kHz and a 30 s repetition delay while the ^{27}Al MAS NMR spectra are recorded with ^{1}H high-power decoupling, ν_R = 13.0 kHz, and a 2 s repetition delay.

5. Synchrotron powder diffraction

In-situ powder X-ray diffraction experiments were carried out on Station 6.2 at the UK Synchrotron Radiation Source (SRS). We use a monochromated beam at a wavelength of 1Å to give optimum sample penetration and data quality. The medium-high resolution curved 1-

dimensional wide-angle X-ray scattering (WAXS) RAPID2 detector is capable of handling the very high intensity diffracted X-rays without attenuating the incident beam and has an acceptance angle of 35 to 95 °2θ.

At the centre of rotation of the 2θ arm we have mounted a capillary heater, similar in design to that of Norby [32]. Wet samples are mixed externally and loaded into 1mm dia quartz glass capillaries with 0.02 mm wall thickness. The capillary is then back pressured at 40 bar with nitrogen gas to prevent loss of water during heating. Finally the capillary is heated, to 200, 225 or 250 °C, with an air heater using a ramp time of 30 min and a hold time of 90 min.

Patterns are collected for 240 x 30 s with a wait time of 1 ms between each pattern. The width of the diffraction peaks of well crystallised components is typically <0.01 nm^{-1} (full-width half-maximum) in 1/*d* reciprocal space. Absolute calibration of *d*-spacings is made with Sigma Aldrich 21561-9 silicon and a correction for the slow decay in synchrotron X-ray intensity during an experiment is made by normalising detector counts within a single experimental shift to constant synchrotron beam current.

Four samples were run to investigate the early hydration times of a 50:50 lime-quartz system (WS=2) from 200 to 250 °C. One sample run at 250 °C was doped with 0.05 g corundum BWOS. Small amounts of contaminant calcite are present in the lime and can be observed as either calcite or scawtite in the final product.

The only sample which produced a crystalline product within 2 h was the alumina-free sample hydrated at 250 °C (Fig. 5). Here we can see the consumption of portlandite and quartz to form xonotlite. Prior to crystalline xonotlite formation there appears to be a precursory gel-like phase with a broad peak at 3.22 nm^{-1} (0.31 nm). All the other samples displayed this same precursory gel-like phase but no crystalline secondary phases were observed.

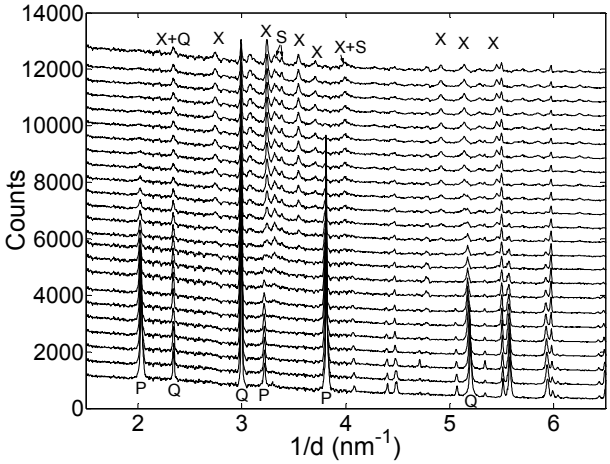

Fig 5. Synchrotron XRD patterns for 50:50 lime and quartz hydrated at 250 °C. Patterns shown were collected every 5 min. Key: P=portlandite, Q=quartz, S=scawtite, X=xonotlite.

If the peak areas of the major peaks are plotted versus time we can start to understand the relative rates of reaction in the system (Fig. 6). Both portlandite and quartz decrease non-linearly over time. The most obvious control on the dissolution of the starting products is temperature whereby dissolution occurs more slowly at lower temperatures and faster at higher temperatures. The addition of alumina does not appear to affect the dissolution rate of portlandite but does increase the dissolution rate of quartz in the first hour. A more rapid dissolution rate might be expected to produce secondary hydrates faster but this is not the case here. As previously mentioned no secondary hydrates were observed when alumina was added to the system.

6. Conclusions

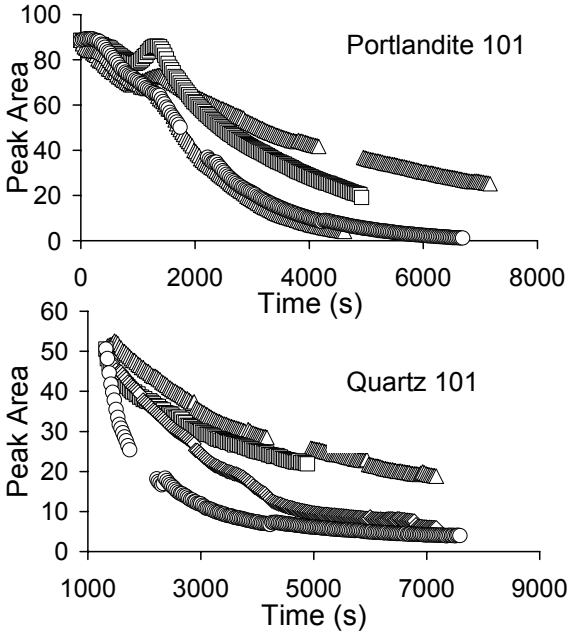

Fig. 6. Peak Area vs hydration time for 50:50 portlandite and quartz mixes. Key: triangles=200 °C, squares=225 °C, diamonds=250 °C, circles=250 °C with 0.05 corundum BWOS.

Although in its preliminary stages, a number of important conclusions can be drawn from this work. (*i*) The use of different initial reactants gives different phase assemblages after 5 days curing. This may be due to different rates of reaction of different starting products and will be examined further with real time investigations using synchrotron diffraction. (*ii*) Phases observed in our system have not been observed in those of others at these temperatures. More work is required to establish whether these phases are metastable or if some phase stability fields need to be re-established. (*iii*) Al-doping of the C-S-H system appears to have three effects. The first is to stabilise phases outside their normal stability field, e.g. 11Å tobermorite. Whether such phases are truly stable or are metastable remains unknown. Second the Al may reside in nominally Al-free calcium silicate hydrates, e.g. xonotlite, kilchoanite, but not significantly affect or slightly reduce their stability. Lastly the presence of alumina appears to prevent the formation of phases completely, e.g. foshagite. Further investigation is required to establish whether Al can be a guest ions in other phases identified in the C-S-H system to date. (*iv*) The presence of aluminium guest-ions in 11Å tobermorite is confirmed by

^{27}Al and ^{29}Si NMR spectroscopy. (*v*) In early stage hydration (<2 h) of 50:50 lime quartz mixes alumina appears to increase dissolution rates of quartz but inhibits formation of crystalline secondary phases.

Finally the engineering implications of Al guest ions in nominally aluminium free calcium silicate hydrates is as yet unknown. The presence of tobermorite in well sealants is often cited as advantageous due to improved strength and impermeability. However the forced doping of calcium silicate hydrates may or may not be detrimental to such qualities by e.g. weakening the crystal structure. Hence although the results both of previous authors and this study have potential benefits for sealant design the results should be treated with caution until we know if we are altering the crystal structure in such a way that a sealant containing such phases could prove deleterious. This will be the subject of future investigations.

Acknowledgements

We thank EPSRC for funding this research, Chris Martin, Graham Clark, Alfie Nield and Dave Kinder at the UK Synchrotron Source, Bobby Hogg, Bill Leslie and Dave Archibald at the University of Edinburgh and Ian Madsen and Nikki Scarlett of CSIRO, Australia. The use of the facilities at the Instrument Centre for Solid-State NMR Spectroscopy, sponsored by the Danish Natural Science Research Councils is acknowledged.

References

[1] G. Carter and D. K. Smith, Properties of cementing compositions at elevated temperatures and pressure, Trans Metal Soc American Inst Metal Eng 213 (1958) 20-27
[2] E. Nelson, Thermal Cements, in: E. Nelson (Eds.), Well Cementing, Schlumberger Educational Services, Sugar Land, Texas, 1990, pp.
[3] H. F. W. Taylor, The Calcium Silicate Hydrates, in: H. F. W. Taylor (Eds.), The Chemistry of Cements, Academic Press, London, 1964, pp. 168-232
[4] N. Meller and C. Hall, Hydroceramic sealants for geothermal wells, in M. Pecchio, F. R. D. Andrade, L. Z. D. D'Agostino, H. Kahn, L. M. Sant'Agostigno and M. M. M. L. Tassinari (Eds) International Congress on Applied Mineralogy, Internation Council for Applied Mineralogy do Brasil, 2004, 281-284.
[5] N. Meller, C. Hall and J. Phipps, A new phase diagram for the CaO-$Al2O_3$-SiO_2-H_2O hydroceramic system at 200°C, Mat Res Bull 40 (2005) 715-723
[6] N. Meller, K. Kyritsis, G. Giriat and C. Hall, Synthesis of cement based CaO-Al_2O_3-SiO_2-H_2O (CASH) hydroceramics at 200 and 250^o C: Ex-situ and in-situ diffraction, Cem Conc Res (in press)

[7] V. Barlet-Gouédard and B. Vidick, A non-conventional way of developing cement slurry for geothermal wells, Geothermal Resources Council Transactions 25 (2001) 85-91
[8] A. L. Mackay and H. F. W. Taylor, Truscottite, Min Mag 30 (1954) 450-457
[9] S. Merlino, Gyrolite: its crystal structure and crystal chemistry, Min Mag 52 (1988) 377-387
[10] J. J. Esteban, J. Cuevas and J. M. Tubia, Xonotlite in rodingite assemblages from the Ronda Peridotites, Betic Cordilleras, southern Spain, Can Mineral 41 (2003) 161-170
[11] G. L. Kalousek and S. L. Chow, Research on cements for geothermal and deep oil wells, Soc Pet Eng of AIME SPE 5940 (1976)
[12] T. Sugama, L. E. Kukacka and W. Horn, Effects of tobermorite and calcium silicate hydrate (I) crystals formed within polymer concretes, J Mat Sci 16 (1980) 345-354
[13] N. Isu, H. Ishida and T. Mitsuda, Influence of quartz particle size on the chemical and mechanical properties of autoclaved aerated concrete (I) Tobermorite formation, Cem Conc Res 25 (1995) 243-248
[14] D. S. Klimesch and A. S. Ray, DTA_TG study of the CaO-SiO_2-H_2O and CaO-Al_2O_3-SiO_2-H_2O systems under hydrothermal conditions, J Thermal Analysis and Calorimetry 56 (1999) 27-34
[15] D. S. Klimesch and A. S. Ray, Effect of quartz content on the nature of Al-substituted 11A tobermorite in hydrothermally treated CaO-Al_2O_3-SiO_2-H_2O systems, Adv Cem Res 11 (1999) 179-187
[16] F. Liu, D. Chen, W. Ni and Z. Cao, Effect of Al3+ on tobermorite crystallinity, Journal of University of Science and Technology Beijing 7 (2000) 79-81
[17] S. Shaw, S. M. Clark and C. M. B. Henderson, Hydrothermal formation of the calcium silicate hydrates, tobermorite ($Ca_5Si_6O_{16}(OH)_2.4H_2O$) and xonotlite ($Ca_6Si_6O_7(OH)_2$): an in-situ synchrotron study, Chem Geol 167 (2000) 12-140
[18] L. D. Sanders and W. J. Smothers, Effect of tobermorite on the mechanical strength of autoclaves Portland cement-silica mixtures, J Am Conc Inst 28 (1957) 127-134
[19] S. Merlino, E. Bonaccorsi and T. Armbruster, The real structure of tobermorite 11A: normal and anomalous forms, OD character and polytypic modifications, Eur J Min 13 (2001) 577-590
[20] S.-Y. Hong and F. Glasser, Phase relations in the CaO-SiO_2-H_2O system to 200 °C at saturated steam pressure, Cem Conc Res 34 (2004) 1529-1534
[21] K. Garbev, L. Black, G. Beuchle and P. Stemmermann, Inorganic Polymers in Cement Based Materials, Wasser und Geotechnologie 2 (2002) 19-30
[22] K. Yanagisawa, X. Hu, A. Onda and K. Kajiyoshi, Hydration of β-dicalcium silicate at high temperatures under hydrothermal conditions, Cem Conc Res 36 (2006) 810-816

[23] X. Hu, K. Yanagisawa, A. Onda and K. Kajiyoshi, Effects of Hydrothermal Process on Formation of calcium Silicate Hydrates at 250 °C, J Soc Inorg Mat, Japan 13 (2006) 32-39
[24] X. Hu, K. Yanagisawa, A. Onda and K. Kajiyoshi, Stability and phase relations of dicalcium silicate hydrates under hydrothermal conditions, J Ceram Soc Japan 114 (2006) 174-179
[25] P. Barnes, S. L. Colston, A. C. Jupe, S. D. M. Jacques, M. Attfield, R. Pisula, S. Morgan, C. Hall, P. Livesey and S. Lunt, The use of synchrotron sources in the study of cement materials, in: J. Bensted and P. Barnes (Eds.), Structure and Performance of Cements, Spon Press, London & New York, 2002, pp.
[26] M. D. Andersen, H. J. Jakobsen and J. Skibsted, Incorporation of aluminium in the calcium silicate hydrate (C-S-H) of hydrated Portland cements: A high field ^{27}Al and ^{29}Si MAS NMR investigation, Inorg Chem 42 (2003) 2280-2287
[27] M. D. Andersen, H. J. Jakobsen and J. Skibsted, A new aluminium-hydrate species in hydrated Portland cements characterized by ^{27}Al and ^{29}Si MAS NMR spectroscopy, Cem Conc Res 36 (2006) 3-17
[28] G. M. M. Bell, J. Bensted, F. P. Glasser, E. E. Lachowski, D. R. Roberts and M. J.-. Taylor, Study of calcium silicate hydrates by solid-state high-resolution ^{29}Si nuclear magnetic resonance, Adv Cem Res 9 (1990) 23-37
[29] R. Gabrovsek, B. Kurbus, D. Mueller and W. Wiker, Tobermorite formation in the system CaO, C_3S-SiO_2-AlO_3-NaOH-H_2O under hydrothermal conditions, Cem Conc Res 23 (1993) 321-328
[30] X. Cong and R. J. Kirkpatrick, 29Si and 17O NMR Investigation of the Structure of Some Crystalline Calcium Silicate Hydrates, Adv Cem Based Mat 3 (1996) 133-143
[31] M. R. Hansen, H. J. Jakobsen and J. Skibsted, ^{29}Si chemical shift anisotropies in calcium silicates from high-field ^{29}Si MAS NMR spectroscopy, Inorg Chem 42 (2003) 2368-2377
[32] P. Norby, Hydrothermal conversion of zeolites: An in-situ synchrotron X-ray powder diffraction study, J Am Chem Soc 119 (1997) 5215-5221